Peer-reviewed version available at Micromachines 2018, 9, 607; doi:10.3390/mi9110607

Self-renewal and Differentiation of Adipose-derived Stem Cells (ADSCs) Stimulated by Multi-axial Tensile Strain in a Pneumatic Microdevice

Chih-Hao Chiu [1, 2], Yun-Wen Tong [1], Wen-Ling Yeh [2, 3], Kin Fong Lei [4, 5, *], Alvin Chao-Yu Chen [2, 3, *]

[1] Department of Orthopedic Surgery, Chang Gung Memorial Hospital, Taoyuan, 333 Taiwan

[2] Bone and Joint Research Center, Chang Gung Memorial Hospital, Linkou, 333 Taiwan

[3] Department of Orthopedic Surgery, Chang Gung Memorial Hospital, Linkou, 333 Taiwan

[4] Graduate Institute of Biomedical Engineering, Chang Gung University, Taoyuan, 333 Taiwan

[5] Department of Radiation Oncology, Chang Gung Memorial Hospital, Linkou, 333 Taiwan

* Corresponding authors: Kin Fong Lei; Alvin Chao-Yu Chen

E-mail: kflei@mail.cgu.edu.tw (K.F. Lei); alvinchen@cgmh.org.tw (A.C.Y. Chen)

Tel: +886-3-2118800 ext 5345 (K.F. Lei); +886-3-3281200 ext 3882 (A.C.Y. Chen)

Abstract

Adipose-derived stem cells (ADSCs) were suggested for treating degenerative osteoarthritis, suppressing inflammatory responses, and repairing damaged soft tissues. Moreover, the ADSCs have the potential to undergo self-renewal and differentiate into bone, tendon, cartilage, and ligament. Recently, investigation of the self-renewal and differentiation of the ADSCs becomes an attractive area. In this work, a pneumatic microdevice has been developed to study the gene expression of the ADSCs after the stimulation of multi-axial tensile strain. The ADSCs were cultured on the microdevice and experienced multi-axial tensile strain during a 3-day culture course. Self-renewal and differentiation abilities were investigated by mRNA expressions of NANOG, SOX2, OCT4, SOX9, PPAR-γ, and RUNX2. The result showed that the genes related self-renewal were significantly up-regulated after the tensile stimulation. Higher proliferation ratio of the ADSCs was also shown by cell viability assay. The microdevice provides a promising platform for cell-based study under mechanical tensile stimulation.

Keywords: Microdevice; Tensile stimulation; Adipose-derived stem cells; Self-renewal; Differentiation.

Peer-reviewed version available at Micromachines 2018, 9, 607; doi:10.3390/mi9110607

1. Introduction

Tendon and ligament injuries induce serious consequences such as debilitating pain and reduced joint function. The rotator cuff repairs are conducted over 250,000 times in North American each year. High re-tear rate is still occurred in spite of newly developed techniques are adopted to increase the repair strength [1-4]. Thus, numerous methods had been proposed to enhance tendon healing including stem cells, mechanical forces, pulsed electromagnetic fields (PEMFs), drugs, gene therapy, osteoconductive materials, cell-based therapy, biodegradable scaffolds, low-intensity pulsed ultrasound treatment, and biomimetic patches [4-12]. The use of human stem cells is one of the popular research approaches for soft tissue healing. In the past decade, adipose-derived stem cells (ADSCs) were suggested to be adult stem cell population isolated from adipose tissue [13, 14]. The largest study of using adipose-derived stromal vascular fraction cells (SVF cells) to treat osteoarthritis involved 1128 patients [15]. Most cases consistently reported that adipose-derived cell therapy for treating degenerative osteoarthritis is safe and effective. Moreover, some reports revealed the ADSCs contain unique populations of cells that suppress the inflammatory responses, and thus may further contribute to tissue regeneration and repair of damaged tendon tissues [16, 17]. A review article summarized the ADSCs could be used for the regeneration of damaged tissues [18]. In addition, because stem cells are known as multipotent, nonhematopoietic stromal cells that have the potential to undergo self-renewal, they have the ability to differentiate into bone, tendon, cartilage, and ligament [19-22].

In the literatures, much of the work has focused on human bone marrow mesenchymal stem cells (MSCs). Mechanical stretching was shown to induce the proliferation and differentiation of MSCs into tenocytes associated with cumulative elongation [23, 24]. MSC-to-tenocyte under 3%-10% mechanical stretching at 1 Hz was evaluated by analyzing mRNA expression levels [25, 26]. Studies have shown that

Peer-reviewed version available at Micromachines 2018, 9, 607; doi:10.3390/mi9110607

applying intermittent mechanical tension to MSCs (every few hours, several times a day, for several days) promotes osteogenic differentiation, whereas applying continuous mechanical tension to MSCs inhibits osteogenic differentiation. On the other hand, osteogenic differentiation of the ADSCs was reported to be induced under uniaxial stretching [27-29]. Cyclic tensile strain significantly increased gene expressions of BMP2 and BUNX2, which respond for the modulation of the osteogenic differentiation. Also, cyclic tensile strain would lead to more aligned and organized ADSCs. Moreover, a study reported the comparison of ADSCs and MSCs under mechanical stretching [30]. The results concluded that ADSCs are more rapid responders to mechanical stretching and have greater potential than MSCs in osteogenesis. Thus, more and more works have been focused on the investigation of the proliferation and differentiation of ADSCs stimulated by mechanical stretching.

In the above *in vitro* experiments, uniaxial stretching apparatus were used to apply single directional strain to the cells. However, during the movement of the body, the soft tissues are subjected to multi-axial mechanical strain. Development of multi-axial mechanical stretching microdevice is necessary to mimic the native *in vivo* environment. With the mature development of microfabrication technology, a number of microdevices have been developed for various biomedical and clinical applications [31-33]. For example, biological cells have been shown to be cultured in a controlled microenvironment for investigating their physiology and biochemistry under the tested conditions [34, 35]. A microfluidic device composed of 10×10 culture chambers was demonstrated on a high throughput cell-based screening application. Mammalian HeLa cells were cultured in the chamber and proliferated nearly to confluency after 7.5 days to show a promising evidence of microfluidic cell culture model. In these microfluidic devices, one of the commonly used materials is polydimethylsiloxane (PDMS), which is optically transparent, flexible, and bio-compatible. Thus, the PDMS deflective

Peer-reviewed version available at Micromachines 2018, 9, 607; doi:10.3390/mi9110607

membrane could be developed to provide compressive force for cell stimulation [36]. Cell viability was investigated under different levels of compressive force. Nowadays, the PDMS membrane-type microdevices fabricated by microfabrication technology are recognized to be a promising tool for cell-based assays.

In the current work, a PDMS-based microdevice was developed for providing multi-axial mechanical tensile stretching for cell stimulation. The device was composed of 9 culture chambers. The bottom surface of each chamber was a deflective membrane actuated by pneumatic structure. The pressure and actuation frequency were controlled by a microcontroller. ADSCs were cultured on the chamber and experienced multi-axial tensile strain during a 3-day culture course. Self-renewal ability was investigated by mRNA expressions of NANOG, SOX2, and OCT4. Moreover, chondrogenic gene of SOX9, adipogenic gene of PPAR-γ, and osteogenic gene of RUNX2 were analyzed to study the cell differentiation. The result showed that NANOG, SOX2, and OCT4 were significantly up-regulated after the tensile stimulation. Higher proliferation ratio of the ADSCs was also shown by the cell viability assay. That indicated self-renewal of the ADSCs was confirmed after the mechanical stretching.

2. **Materials and methods**

2.1 Harvest and isolation of human ADSCs

Human ADSCs were isolated from discarded tissue of total knee arthroplasty. The approval of the tissue collection was given by the Institutional Review Board at Chang Gung Memorial Hospital, Linkou, Taiwan (IRB No. 2016014923). Seven patients have been recruited for this study and their age and gender are listed in Table 1. Before the surgery, the patients had been given informed consent. The harvested fat tissue is shown in Fig. 1(a). The tissue was digested in enzymatic solution containing 300 U/ml collagenase Type II (Gibco, Invitrogen, Paisley, UK) and cultured at 37°C for 2 h. After

Preprints (www.preprints.org) | NOT PEER-REVIEWED | Posted: 26 September 2018 doi:10.20944/preprints201809.0503.v1

Peer-reviewed version available at Micromachines 2018, 9, 607; doi:10.3390/mi9110607

the digestion process, the solution was filtered and centrifuged at 1,200 rpm for 5 min at room temperature to separate floating mature adipocytes. The cell pellet was then suspended in culture medium (RPMI 1640 supplemented with 10% fetal bovine serum and 1% antibiotics) and maintained in standard culture plates. The microscopic image of the first passage of ADSCs is shown in Fig. 1(b). The ADSCs were confirmed by analyzing the surface markers using flow cytometry, as shown in Fig. 2. The result showed that the ADSCs express CD90+/CD73+/CD105+/CD31-/CD34-/CD45-, that have the phenotypic and functional features of stem cells [21, 22]. The ADSCs above five passages were discarded because of the possibility of phenotypic drift.

Table 1. Summary of the age and gender of the patients.

Patient number	Age	Gender
1	83	Female
2	77	Male
3	69	Female
4	78	Male
5	78	Female
6	63	Female
7	70	Female

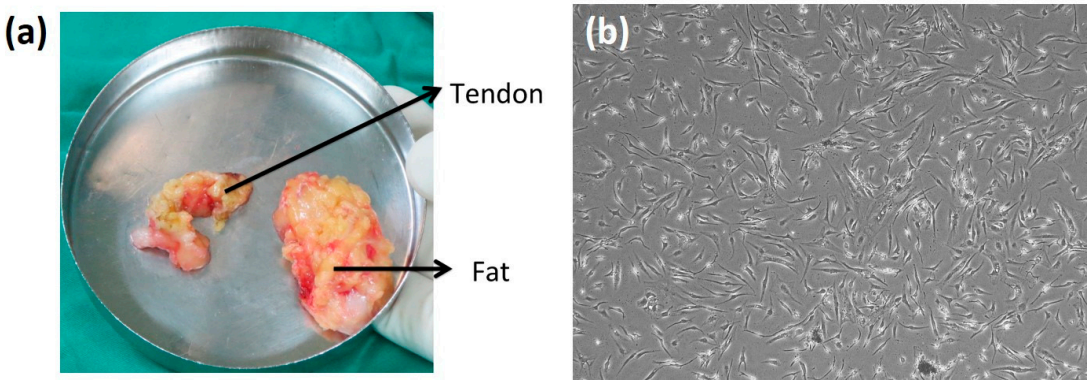

Fig. 1. (a) Photograph of the harvested fat tissue. (b) Microscopic image of the first passage of ADSCs.

Preprints (www.preprints.org) | NOT PEER-REVIEWED | Posted: 26 September 2018 doi:10.20944/preprints201809.0503.v1

Peer-reviewed version available at Micromachines 2018, 9, 607; doi:10.3390/mi9110607

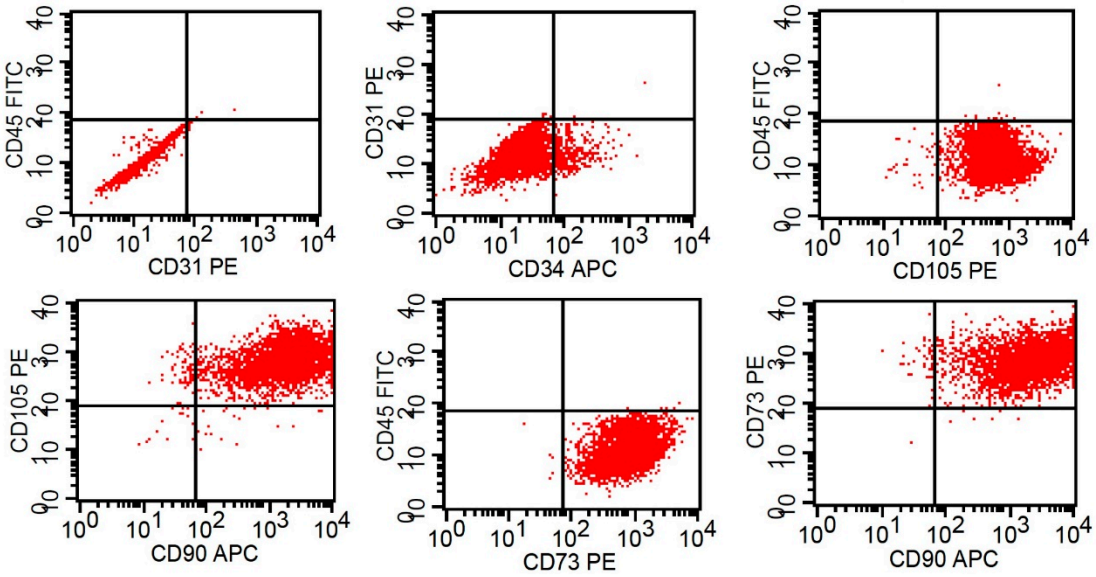

Fig. 2. Analysis of the surface markers of ADSCs by using flow cytometry.

2.2 Fabrication of the microdevice providing multi-axial tensile strain

A PDMS-based microdevice was developed for culturing ADSCs and providing multi-axial tensile strain to the cells. Illustration and photograph of the microdevice are respectively shown in Fig. 3(a) and 3(b). The device consisted of 3 PDMS layers including a culture chamber layer, a membrane, and an air chamber layer. The culture chamber layer was a 5 mm thick PDMS layer with a 3×3 array of circular through holes in the diameter of 10 mm. The membrane was a 100 μm thick PDMS layer. The air chamber layer was composed of a 3×3 array of chambers (1 mm in height) connected with channels. The membrane and the air chamber layer were fabricated by soft lithography. Briefly, poly(methyl methacrylate) (PMMA) molds were respectively fabricated by a micro-engraving machine (EGX-400; Roland, Japan). Afterward, PDMS pre-polymer and curing agent (Sylgard® 184; Dow Corning, USA) in (w/w) 10:1 were manually mixed and degassed in a vacuum chamber. Then, the mixture was poured to the PMMA molds and solidified in an oven at 70 °C for 1 h. Subsequently,

Preprints (www.preprints.org) | NOT PEER-REVIEWED | Posted: 26 September 2018 doi:10.20944/preprints201809.0503.v1

Peer-reviewed version available at Micromachines 2018, 9, 607; doi:10.3390/mi9110607

the PDMS layers were respectively peered off from the molds. Three PDMS layers were bonded by an oxygen plasma (PDC-32G; Harrick Plasma, USA) and placed on a glass substrate for solid support. Therefore, the microdevice with a 3×3 array of culture chambers was fabricated. The bottom surface of each chamber was a deflective membrane, which can be actuated by the pressure change of the air chamber. The pressure and actuation frequency were controlled by an in-house built instrument including a compressed air pump, a pressure gauge, and an electronic valve controlled by a microcontroller. ADSCs were cultured on the chamber and experienced multi-axial tensile strain during culture course. Illustration of the experimental setup is shown in Fig. 3(c).

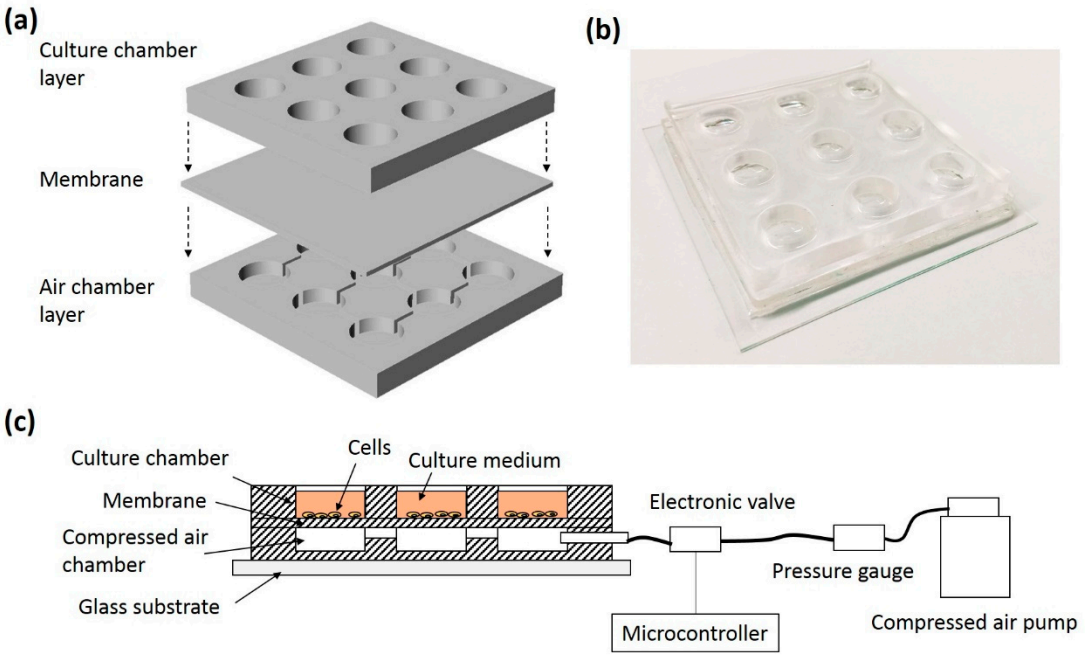

Fig. 3. (a) Illustration of the design of the microdevice. (b) Photograph of the microdevice. (c) Illustration of the experimental setup of the cells stimulated by the multi-axial tensile strain.

2.3 ADSCs cultured on the microdevice

Before the cell culture experiment, the microdevice was sterilized under ultraviolet light overnight. In order to improve cell adhesion on the PDMS surface, 50 μL collagen solution in 50 μg/mL was respectively added to each culture chamber and stored at 4 °C overnight. Then, the culture chambers were washed and ready for the cell culture experiment. 10^5 cells were added to each chamber and cultured in a 37 °C and 5% CO_2 humidified incubator (370; Thermoscientific, USA) overnight. The cells were seeded and spread on the bottom surface, i.e., membrane, of the chamber. After cell stabilization, multi-axial tensile strain at 1 Hz was applied to the cells by applying 5 kPa compressed air to the air chambers. The cells were continuously stimulated for the following 1 or 3 days. Subsequently, the cells were harvested after the culture course and mRNA expression level was examined. Relative gene expression level was defined as the gene expression level with stretching stimulation divided by the gene expression level without stretching stimulation. The change of the gene expression was investigated to evaluate the properties of self-renewal and differentiation.

The deformation of the membrane was quantified by images captured from a microscope installed horizontally. From the images, the height and angle of the deformed membranes were measured using ImageJ computer software. Then, the contour of the deformed membrane, $f(x)$, could be estimated by quadratic equation fitting. The axial elongation, x, was calculated by

$$x = \int_b^a \sqrt{1 + f(x)'}\, dx \quad (1)$$

Thus, the deformation of the membrane could be controlled by the applied pressure. The cells cultured on the membrane received the multi-axial tensile strain during the culture course.

2.4 Investigation of mRNA expressions

Preprints (www.preprints.org) | NOT PEER-REVIEWED | Posted: 26 September 2018 doi:10.20944/preprints201809.0503.v1

Peer-reviewed version available at Micromachines 2018, 9, 607; doi:10.3390/mi9110607

After the culture course, the cells were harvested and mRNA expression was then investigated by using real time polymerase chain reaction (PCR). Briefly, total RNA of the cells was extracted using GENEzol^{TM} TriRNA Pure Kit (GZX100; Geneaid, Taiwan) according to the supplier's instruction. Then, cDNA was synthesized by cDNA synthesis kit (18080-400; Invitrogen, USA) using a T100^{TM} Thermal Cycler (Bio-Rad, USA). The relative quantity of mRNA was determined by a CFX Connect^{TM} Real-time PCR Detection System (Bio-Rad, USA) using TaqMan™ Universal Master Mix II, with UNG (4440038; ThermoFisher Scientific, USA). The mRNA expressions of NANOG, SOX2, OCT4, SOX9, PPAR-γ, and RUNX2 were examined. The TaqMan® gene expression assays were used and are listed in Table 2. The expression of GAPDH was used as the internal control.

Table 2. TaqMan® gene expression assays.

Gene	Assay number (ThermoFisher Scientific, USA)
GAPDH	Hs03929097_g1
NANOG	Hs02387400_g1
SOX2	Hs00602736_s1
OCT4	Hs01895061_u1
SOX9	Hs00165814_m1
PPAR-γ	Hs01115513_m1
RUNX2	Hs00231692_m1

2.5 Quantification of cell proliferation

Number of living cells was quantified by bio-assay such as WST-1 assay (Roach Applied Science, USA). After the culture course, the culture medium was removed and the reagent of WST-1 assay in a dilution of 1:10 (v/v) was added to each chamber. The reagent reacted with the respiratory chain of mitochondria and the color intensity of the reagent changed according to the reaction level. After incubation at 37 °C for 2 h, the

Preprints (www.preprints.org) | NOT PEER-REVIEWED | Posted: 26 September 2018 doi:10.20944/preprints201809.0503.v1

Peer-reviewed version available at Micromachines 2018, 9, 607; doi:10.3390/mi9110607

reacted reagent was collected and quantified by a microplate reader (ELx800; BioTek Instruments, USA) at an absorbance of 440 nm with a reference wavelength of 660 nm. Thus, the color intensity of the reacted reagent could be represented by optical density (OD). The proliferation ratio was defined as the OD value at the end of the culture course divided by the OD value at the beginning of the culture course.

3. **Results and discussion**

3.1 Investigation of the membrane deformation

The deformation of the membrane was induced by the pressure applied to the air chamber. The pressures of 2, 4, 6, 8, and 10 kPa were regulated to induce different levels of deformation. Side view photographs of the deformed membrane were captured under different applied pressures and are shown in Fig. 4(a). The height and angle of the deformed membranes are also indicated in the photographs. Obviously, higher pressure generated larger deformation. Hence, the contours of the deformed membrane were fitted by quadratic equation. The result is shown in Fig. 4(b). The axial elongation and strain were calculated and are listed in Table 3. Correlation between the applied pressure and the axial strain is shown in Fig. 5. A linear correlation with an R-squared value of 0.9780 was obtained. That indicates the deformation of the membrane was in the elastic region. In addition, the axial strain ranging from 0 to 12 % was achieved and that is suitable to the mechanical stretching study for cells.

Table 3. The elongation and strain of the membrane induced by different pressures.

Applied pressure (kPa)	0	2	4	6	8	10
Axial elongation (mm)	10.00	10.38	10.53	10.87	11.00	11.20
Axial strain	0	3.8	5.3	8.7	10	12

Preprints (www.preprints.org) | NOT PEER-REVIEWED | Posted: 26 September 2018 doi:10.20944/preprints201809.0503.v1

Peer-reviewed version available at Micromachines 2018, 9, 607; doi:10.3390/mi9110607

(%)						

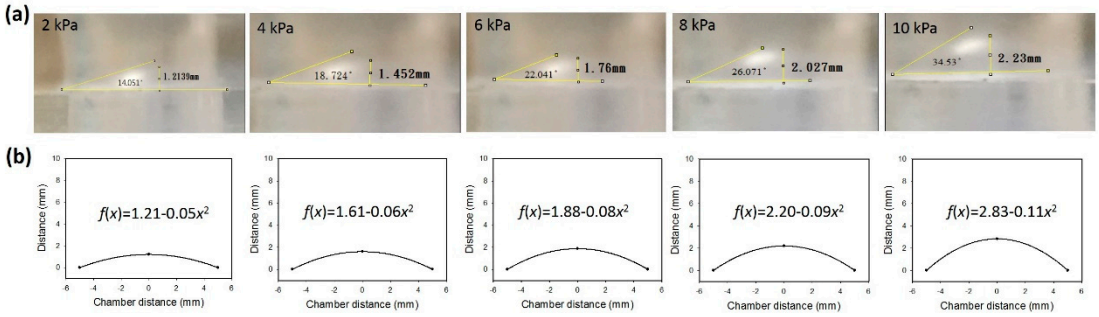

Fig. 4. (a) Side view photographs of the deformed membrane under different applied pressures. (b) Contours of the deformed membrane fitted by quadratic equation.

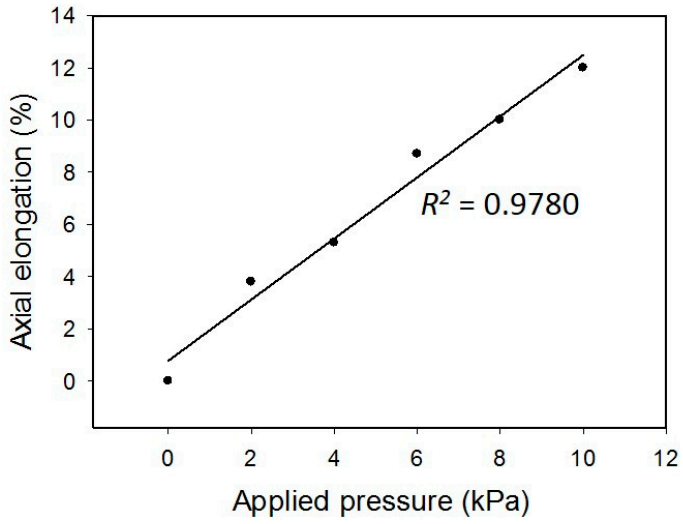

Fig. 5. Correlation between the applied pressure and the axial strain.

3.2 mRNA expressions of cells after mechanical stretching stimulation

In this study, self-renewal genes (NANOG, SOX2, and OCT4), chondrogenic gene (SOX9), adipogenic gene (PPAR-γ), and osteogenic genes (RUNX2) were examined to study the self-renewal and differentiation capacity of the ADSCs after mechanical stretching stimulation. NANOG is a transcription factor in embryonic stem cells and functions with SOX2 and OCT4 to maintain pluripotency [37, 38]. Thus, self-renewal

capacity could be analyzed by NANOG, SOX2, and OCT4. Moreover, transcription factor SOX9 has an essential role during chondrocyte differentiation [39]. PPAR-γ is a member of the nuclear hormone receptor superfamily and has a key role of adipose cell differentiation [40]. RUNX2 was reported to promote osteogenic differentiation [41]. Thus, the multipotential differentiation of the ADSCs was studied by analyzing SOX9, PPAR-γ, and RUNX2.

A control experiment (without mechanical stretching stimulation) was conducted to investigate the gene expression level of the ADSCs. The ADSCs (isolated from the tissue samples of patient #1 and #2) were cultured on the culture chambers for 3 days. Gene expression level was compared before and after the 3-day culture course. Fig. 6 reveals the gene expression was not changed. That indicates the culture environment did not induce the change of the gene expression of the cells. Then, the gene expression of the ADSCs after the stimulation of the multi-axial tensile strain was investigated. The ADSCs (isolated from the tissue samples of patient #1 and #2) were respectively stimulated by the multi-axial tensile strain for 1 day and 3 days. The result is shown in Fig. 7. That revealed NANOG, SOX2, and OCT4 were up-regulated after the stimulation. The result implies that self-renewal capacity of the ADSCs was induced by mechanical stretching. Importantly, the cells stimulated for 3 days had a higher influence than those for 1 day. On the other hand, the gene expressions of SOX9, PPAR-γ, and RUNX2 were not changed and that implies the differentiation of the ADSCs was not induced.

Preprints (www.preprints.org) | NOT PEER-REVIEWED | Posted: 26 September 2018 doi:10.20944/preprints201809.0503.v1

Peer-reviewed version available at Micromachines 2018, 9, 607; doi:10.3390/mi9110607

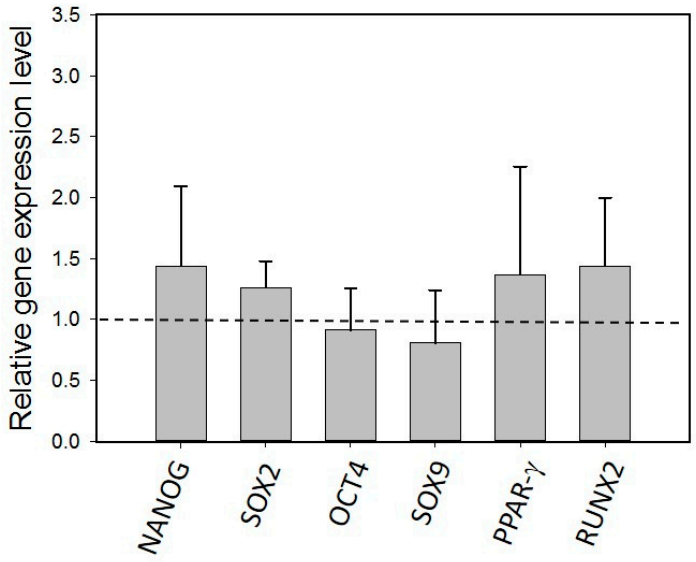

Fig. 6. Control experiment that culturing the ADSCs without mechanical stretching stimulation. Gene expression level was compared before and after a 3-day culture course. The ADSCs were isolated from the tissue samples of patient #1 and #2. The data are presented as mean ± standard error.

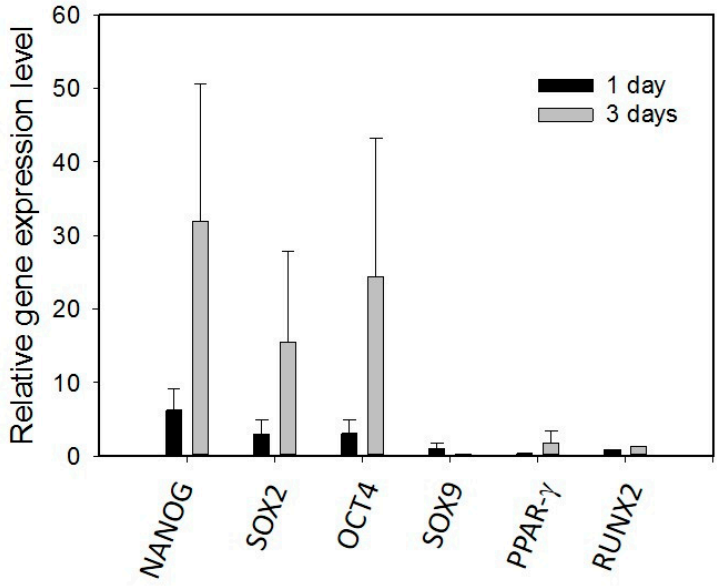

Fig. 7. Investigation of the gene expression of the ADSCs after the stimulation of the multi-axial tensile strain. The ADSCs were respectively stimulated by the multi-axial

Preprints (www.preprints.org) | NOT PEER-REVIEWED | Posted: 26 September 2018 doi:10.20944/preprints201809.0503.v1

Peer-reviewed version available at Micromachines 2018, 9, 607; doi:10.3390/mi9110607

tensile strain for 1 day and 3 days. The ADSCs were isolated from the tissue samples of patient #1 and #2. The data are presented as mean ± standard error.

Because the self-renewal capacity of the ADSCs could be induced by the mechanical stretching, investigation of the cell proliferation was conducted. The ADSCs (isolated from the tissue samples of patient #1 and #2) were stimulated by the multi-axial tensile strain for 3 days. Cell proliferation ratio was quantified and compared with the control group (the cells cultured without stimulation for 3 days). Fig. 8 shows that the proliferation ratio of the stimulated cells was increased. That indicates the mechanical stretching could also enhance cell proliferation. Moreover, microscopic images of the cells with/without stimulation were captured and are shown in Fig. 9. The images show the ADSCs were concentrically aligned due to the stimulation of the multi-axial tensile strain.

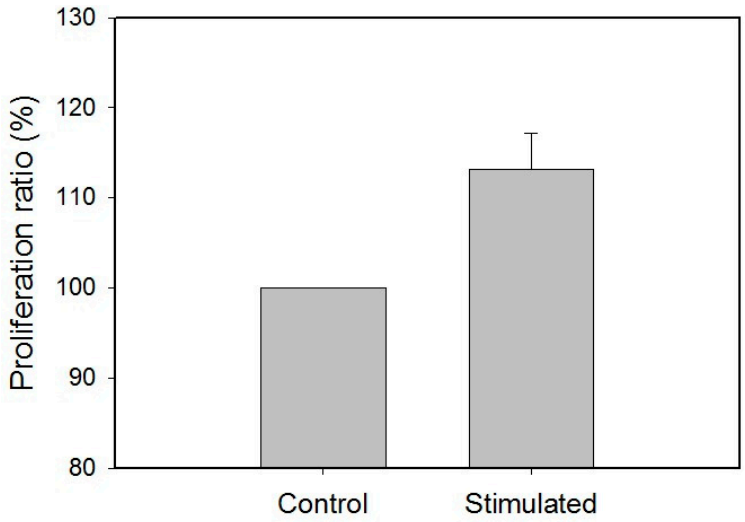

Fig. 8. Investigation of the cell proliferation after the stimulation of the multi-axial tensile strain for 3 days. The ADSCs were isolated from the tissue samples of patient #1 and #2. The data are presented as mean ± standard error.

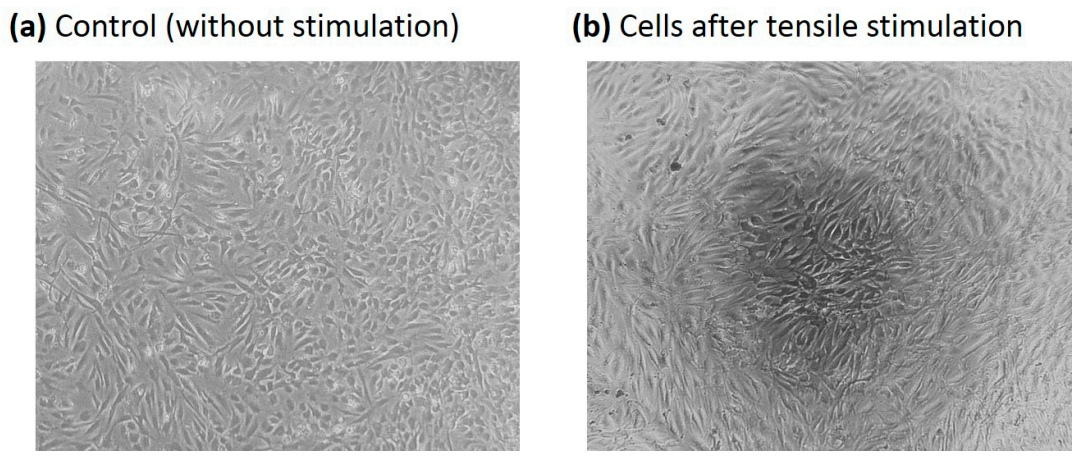

Fig. 9. Microscopic images of the ADSCs. (a) Control group (without stimulation). (b) The cells stimulated by multi-axial tensile strain for 3 days.

3.3 Gene expression influenced by individuals

In the last section, the self-renewal capacity of the ADSCs was shown to be induced by the mechanical stretching. However, individual variability is known to be one of the issues of the influence of gene expression. Thus, more patients were recruited in order to study the individual variability. The ADSCs were respectively stimulated by the multi-axial tensile strain for 3 days and the relative gene expression levels were investigated, as shown in Fig. 10. Distinct outcomes were revealed from the figure. For the ADSCs isolated from patient #1, #2, #3, and #6, the genes related to self-renewal capacity (NANOG, SOX2, and OCT4) were up-regulated and other genes related to differentiation (SOX9, PPAR-γ, and RUNX2) were not changed. In contrast, for the ADSCs isolated from patient #4, #5, and #7, the genes related to differentiation (SOX9, PPAR-γ, and RUNX2) was up-regulated, especially for RUNX2. That implies osteogenic differentiation was promoted. That agrees with the result from the literatures [27-29]. The result shows individual variability highly dominates the outcome of the gene expression after the stimulation.

Preprints (www.preprints.org) | NOT PEER-REVIEWED | Posted: 26 September 2018 doi:10.20944/preprints201809.0503.v1

Peer-reviewed version available at Micromachines 2018, 9, 607; doi:10.3390/mi9110607

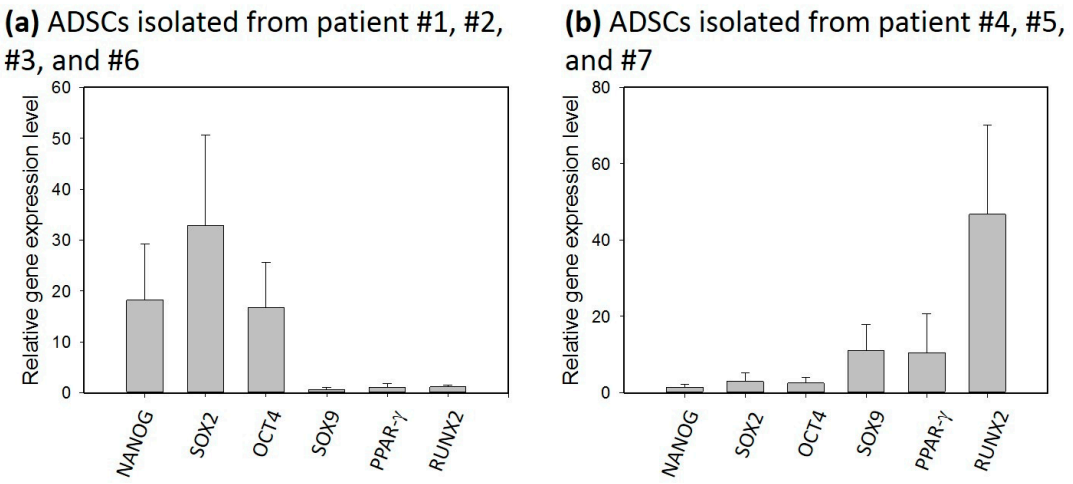

Fig. 10. Investigation of the gene expression of the ADSCs after the stimulation of the multi-axial tensile strain. (a) The ADSCs were isolated from patient #1, #2, #3, and #6. (b) The ADSCs were isolated from patient #4, #5, and #7. The ADSCs were respectively stimulated by the multi-axial tensile strain for 3 days. The data are presented as mean ± standard error.

4. Conclusions

A PDMS-based microdevice has been developed to study the gene expression of the ADSCs after the stimulation of multi-axial tensile strain. The results indicated that the gene expressions of NANOG, SOX2, and OCT4 were up-regulated, while SOX9, PPAR-γ, and RUNX2 were not changed after the stimulation. Importantly, the cells stimulated for 3 days had a higher influence than those for 1 day. Also, proliferation of the ADSCs was increased by the mechanical stretching. That implied self-renewal capacity of the ADSCs was shown to be induced. However, the result was highly influenced by the individual variability. Another set of the ADSCs isolated from the other patients showed osteogenic differentiation was promoted after the stimulation.

Nevertheless, the microdevice provides a promising platform for the study of ADSCs stimulated by multi-axial tensile strain.

Funding: This study was supported by Chang Gung Memorial Hospital, Linkou, Taiwan (Project number: CMRPG5G0141), AO Trauma (Project number: AOTAP17-03), and Ministry of Science and Technology, Taiwan (Project number: MOST106-2314-B-182A-028).

Conflicts of Interest: The authors declare no conflict of interest.

References:

1 Cole, B.J.; ElAttrache, N.S.; Anbari, A. Arthroscopic rotator cuff repairs: an anatomic and biomechanical rationale for different suture-anchor repair configurations. *Arthroscopy* **2007**, 23, 662–669.

2 Tashjian, R.Z.; Hollins,A.M.; Kim, H.M.; Teefey, S.A.; Middleton, W.D.; et al. Factors affecting healing rates after arthroscopic double-row rotator cuff repair. *Am. J. Sport. Med*. **2010**, 38, 2435-2442.

3 Toussaint, B.; Schnaser, E.; Bosley, J.; Lefebvre, Y.; Gobezie, R. Early structural and functional outcomes for arthroscopic double-row transosseous-equivalent rotator cuff repair. *Am. J. Sport. Med.* **2011**, 39, 1217-1225.

4 Gulotta, L.V.; Kovacevic, D.; Ehteshami, J.R.; Dagher, E.; Packer, J.D.; et al. Application of bone marrow-derived mesenchymal stem cells in a rotator cuff repair model. *Am. J. Sports Med*. **2009**, 37, 2126-2133.

5 Everts, P.A.; Overdevest, E.P.; Jakimowicz, J.J.; Oosterbos, C.J.; Schönberger, J.P.; et al. The use of autologous platelet-leukocyte gels to enhance the healing process in surgery, a review. *Surg. Endosc.* **2007**, 21, 2063-2068.

6 Beck, J.; Evans, D.; Tonino, P.M.; Yong, S.; Callaci, J.J. The biomechanical and histologic effects of platelet-rich plasma on rat rotator cuff repairs. *Am. J. Sports Med.* **2012**, 40, 2037-2044.

7 Chiu, C.H.; Lei, K.F.; Yeh, W.L. Development of a co-culture device for the study of human tenocytes in response to the combined stimulation of electric field and platelet rich plasma (PRP). *Biomed. Microdevices* **2017**, 19, 69.

8 D.R. Carter, P.R. Blenman and G.S. Beaupré, Correlations between mechanical stress history and tissue differentiation in initial fracture healing, *J. Orthop. Res.* **1988**, 6, 736-748.

9 Chiu, C.H.; Liu, J.L.; Chang, C.H.; Lei, K.F.; Chen, A.C.Y. Investigation of osteogenic activity of primary rabbit periosteal cells stimulated by multi-axial tensile strain. *Biomed. Microdevices* **2017**, 19, 13.

10 Brook, J.; Dauphinee, D.M.; Korpinen, J.; Rawe, I.M. Pulsed radiofrequency electromagnetic field therapy: A potential novel treatment of plantar fasciitis. *J. Foot Ankle Surg*. **2012**, 51, 312-316.

11 De Girolamo, L.; Stanco, D.; Galliera, E.; Vigano, M.; Colombini, A.; et al. Low frequency pulsed electromagnetic field affects proliferation, tissue-specific gene expression, and cytokines release of human tendon cell. *Cell Biochem. Biophys*. **2013**, 66, 697-708.

12 Jorgensen, T.E. Electrical stimulation of human fracture healing by means of a slow pulsating, asymmetrical direct current. *Clin. Orthop. Relat. R.* **1977**, 124, 124-127.

13 Zhu, Y.; Liu, T.; Song, K.; Fan, X.; Ma, X.; et al. Adipose-derived stem cell: a better stem cell than BMSC. *Cell Biochem. Funct* **2008**, 26, 664-675.

14 Zuk, P.A. the adipose-derived stem cell: looking back and looking ahead. *Mol. Biol. Cell* **2010**, 21, 1783-1787.

15 Michalek, J.; Moster, R.; Lukac, L.; Proefrock, K.; Petrasovic, M.; et al. Autologous adipose tissue-derived stromal vascular fraction cells application in patients with osteoarthritis. *Cell Transplant* **2015**, doi: 10.3727/096368915X686760.

16 Strioga, M.; Viswanathan, S.; Darinskas, A.; Slaby, O.; Michalek, J. Same or not the same? Comparison of adipose tissue-derived versus bone marrow-derived mesenchymal stem and stromal cells. *Stem Cells Dev.* **2012**, 21, 2724-2752.

17 Varma, M.J.O.; Breuls, R.G.M.; Schouten, T.E.; Jurgens S.J.F.M.; Bontkes, H.Y.; et al. Phenotypical and functional characterization of freshly isolated adipose tissue-derived stem cells. *Stem Cells Dev.* **2007**, 16, 91-104.

18 Parker, A.M.; Katz, A.J. Adipose-derived stem cells for the regeneration of damaged tissues. *Expert Opin. Biol. Ther.* **2006**, 6, 567-578.

19 Beitzel, K.; McCarthy, M.B.; Cote, M.P.; Chowaniec, D.; Falcone, L.M.; et al. Rapid isolation of human stem cells (connective progenitor cells) from the distal femur during arthroscopic knee surgery. *Arthroscopy* **2012**, 28, 74-84.

20 Vangsness, C.T.; Farr, J.; Boyd, J.; Dellaero, D.T.; Mills, C.R.; et al. Adult human mesenchymal stem cells delivered via intra-articular injection to the knee following partial medial meniscectomy: a randomized, double-blind, controlled study. *J. Bone Joint Surgery* **2014**, 96, 90-98.

21 Strem, B.M.; Hicok, K.C.; Zhu, M.; Wulur, I.; Alfonso, Z.; et al. Multipotential differentiation of adipose tissue-derived stem cells. *Keio J. Med*. **2005**, 54, 132-141.

22 Zuk, P.A.; Zhu, M.; Ashjian, P.; De Ugarte, D.A.; Huang, J.I.; et al. Human adipose tissue is a source of multipotent stem cells. *Mol. Biol. Cell* **2002**, 13, 4279-4295.

23 Morita, Y.; Watanabe, S.; Ju, Y.; Xu, B. Determination of optimal cyclic uniaxial stretches for stem cell-to-tenocyte differentiation under a wide range of

mechanical stretch conditions by evaluating gene expression and protein synthesis levels. *Acta Bioeng. Biomechanics* **2013**, 15, 71-79.

24 Altman, G.H.; Horan, R.L.; Martin, I.; Farhadi, J.; Stark, P.; et al. Cell differentiation by mechanical stress. *FASEB J.* **2002**, 16, 270-272.

25 Chen, C.H.; Cao, Y.; Wu, Y.F.; Bais, A.J.; Gao, J.S.; et al. Tendon healing in vivo: gene expression and production of multiple growth factors in early tendon healing period. *J. Hand Surgery* **2008**, 33, 1834-1842.

26 Shi, Y.; Li, H.; Zhang, X.; Fu, Y.; Huang, Y.; et al. Continuous cyclic mechanical tension inhibited Runx2 expression in mesenchymal stem cells through RhoA-ERK1/2 pathway. *J. Cell Physiol.* **2011**, 226, 2159-2169.

27 Yang, X.; Gong, P.; Lin, Y.; Zhang, L.; Li, X.; et al. Cyclic tensile stretch modulates osteogenic differentiation of adipose-derived stem cells via the BMP-2 pathway. *Arch. Med. Sci*. **2010**, 6, 152-159.

28 Rabbani, M.; Janmaleki, M.; Tafazzoli-Shadpour, M.; Teymoori, M.; Rezvaninejad, S. Effects of uniaxial cycle stretch loading on morphology of adipose derived stem cells. *Tissue Eng. Regen. Med*. **2016**, 13, 396-402.

29 Hanson, A.D.; Marvel, S.W.; Bernackl, S.H.; Banes, A.J.; Van Aalst, J.; et al. Osteogenic effects of rest inserted and continuous cyclic tensile strain on hASC lines with disparate osteodifferentiation capabilities. *Annals Biomed. Eng*. **2009**, 37, 955-965.

30 Grottkau, B.E.; Yang, X.; Zhang, L.; Ye, L.; Lin, Y. Comparison of effects of mechanical stretching on osteogenic potential of ASCs and BMSCs. *Bone Res.* **2013**, 3, 282-290.

31 Lei, K.F. Microfluidic systems for diagnostic applications: a review. JALA 2012, 17, 330-347.

32 Lei, K.F. Recent developments and patents on biological sensing using

nanoparticles in microfluidic systems. *Recent Pat. Nanotechnology* **2013**, 7, 81-90.

33 Lei, K.F. Review on impedance detection of cellular responses in micro/nano environment. *Micromachines* **2014**, 5, 1-12.

34 Mehling, M.; Tay, S. Microfluidic cell culture. *Curr Opin Biotech* **2014**, 25, 95-102.

35 Hung, P.J.; Lee, P.J.; Sabounchi, P.; Aghdam, N.; Lin, R.; et al. A novel high aspect ratio microfluidic design to provide a stable and uniform microenvironment for cell growth in a high throughput mammalian cell culture array. *Lab Chip* **2005**, 5, 44-48.

36 Kim, Y.C.; Kang, J.H.; Park, S.J.; Yoon, E.S.; Park, J.K. Microfluidic biomechanical device for compressive cell stimulation and lysis. *Sens Actuators B* **2007**, 128, 108-116.

37 Mitsui, K.; Tokuzawa, Y.; Itoh, H.; Segawa, K.; Murakami, M.; et al. The homeoprotein Nanog is required for maintenance of pluripotency in mouse epiblast and ES cells. *Cell* **2003**, 113, 631–642.

38 Chambers, I.; Colby, D.; Robertson, M.; Nichols, J.; Lee, S.; et al. Functional expression cloning of Nanog, a pluripotency sustaining factor in embryonic stem cells. *Cell* **2003**, 113, 643–655.

39 Akiyama, H.; Chaboissier, M.C.; Martin, J.F.; Schedl, A.; de Crombrugghe, B. The transcription factor SOX9 has essential roles in successive steps of the chondrocyte differentiation pathway and is required for expression of SOX5 and SOX6. *Gens. & Dev.* **2002**, 16, 2813-2828.

40 Spiegelman, B.M. PPAR-gamma: adipogenic regulator and thiazolidinedione receptor. *Diabetes* **1998**, 47, 507-514.

41 Shakibaei, M.; Shayan, P.; Busch, F.; Aldinger, C.; Buhrmann, C.; et al.

Resveratrol mediated modulation of Sirt-1/Runx2 promotes osteogenic differentiation of mesenchymal stem cells: potential role of Runx2 deacetylation. *PLoS one* **2012**, 7, e35712.